Molecular motion and mobility in an organic single crystal: Raman study and model

Z. Q. Ren,[1,*] L. E. McNeil,[1] Shubin Liu,[2] and C. Kloc[3]
[1]*Department of Physics and Astronomy, University of North Carolina at Chapel Hill, Chapel Hill, North Carolina 27599-3255, USA*
[2]*Division of Research Computing, Information Technology Services, University of North Carolina at Chapel Hill, Chapel Hill, North Carolina 27599-3455, USA*
[3]*School of Materials Sciences and Engineering, Nanyang Technological University, Singapore 639798, Singapore*
(Received 31 August 2009; revised manuscript received 4 November 2009; published 17 December 2009)

We report Raman spectra of the organic semiconductor 5,6,11,12-tetraphenyltetracene (rubrene) in the temperature range 30–300 K. The linewidths of certain low-frequency peaks increase significantly, especially in the range 150–200 K. These peaks correspond to the vibrations of the phenyl side groups of the rubrene molecules, and their couplings to intermolecular vibrational modes. We propose a model in which the strong increase in mobility observed with increasing temperature between 30 and 150 K results from disorder as the phenyl groups exchange sides of the backbone plane and break the symmetry. This model explains previous experimental observations of structural and calorimetric changes near 150 K.

DOI: 10.1103/PhysRevB.80.245211 PACS number(s): 78.30.−j, 72.80.Le

I. INTRODUCTION

All-organic devices have drawn a lot of interest over the past decades. Especially since the first organic light-emitting device (OLED) and organic field-effect transistor (OFET) were successfully fabricated,[1,2] many studies and reviews have been conducted on them.[3–7] Compared to liquid crystal display technology, organic transistors and discrete LED displays hold the potential for devices with improved characteristics, including lower power requirements, better resolution, more mechanical flexibility, and lower production costs. Among the organic materials, oligoacenes and their derivatives have an important position in fundamental physics research because the molecules are relatively small and simple, which facilitates understanding of the relationships among molecular structures, optical properties, and transport properties in organics. Once these connections are well understood, it will be possible to tailor molecules for desired performance in devices.

5,6,11,12-tetraphenyltetracene, also known as rubrene, is an oligoacene derivative. Rubrene has an almost 100% photoluminescent yield[8] and has been used in devices such as chemical sensors[9] and actinometers[10] as well as OLEDs (Refs. 11 and 12) and OFETs. Carrier mobility is a fundamental parameter governing charge transport of materials, and at the same time it is crucial for the working efficiency of the end products for most applications. Researchers have found the value of the hole mobility in rubrene single crystals in an FET structure with free-space gate dielectrics to be as high as 30 and 20 cm^2/Vs at low and room temperatures, respectively;[5,13] the maximum mobility of carriers that penetrate deeper into the crystal reaches even 40 cm^2/Vs at room temperature.[14] With other gate materials, e.g., ionic-liquid electrolytes, the mobility reaches up to 9.5 cm^2/Vs,[15] and measurements of Hall mobility yield nearly 10 cm^2/Vs.[16] Although values vary with different configurations and along different crystal axes, they are much higher than those of other organics that share similar molecular structures, such as tetracene (1 cm^2/Vs),[7] and even that of amorphous hydrogenated silicon. Furthermore, different groups report different absolute values of the mobility at various temperatures but in all measurements the mobility increases rapidly from low temperature to ~150–175 K, above which it decreases gradually as the temperature increases further.[5,7] As a comparison, in pentacene, another organic crystal with similar molecular structure, the carrier mobility decreases gradually from low to room temperature,[17,18] which is consistent with a band model for charge transport.[19] In tetracene the carrier mobility increases rapidly from low temperature to ~180 K, and then falls gradually up to room temperature.[7] This behavior is ascribed to a phase transition observed near the temperature at which the mobility has its maximum.[20] However, there has been no x-ray evidence suggesting that such a phase transition occurs in rubrene in the 100–300 K temperature range,[21] and room-temperature polarized Raman spectra on various surfaces of the crystal revealed no multiphase coexistence.[22] Some claim that the mobility drop in the crystal below 140 K could be caused by trapping of carriers by shallow traps,[5,7] and another possible explanation proposed by Li *et al.*[23] suggests that the enhancement of the effective mass of quasiparticles in molecular-orbital bands may be responsible ($\mu = e\tau/m^*$). In this work we present the low-temperature Raman spectra of rubrene single crystals, together with a model to explain how the change in the carrier mobility with temperature and other phenomena observed in crystalline rubrene result from vibrational disorder of the rubrene molecules.

II. EXPERIMENT AND SIMULATION

The single crystals used in these measurements were grown at Bell Laboratories by horizontal physical vapor transport in a flow of argon gas from rubrene powder acquired from Aldrich. The details of this growth process have been described elsewhere.[24] Raman spectra were recorded using a Dilor XY triple spectrometer in a backscattering configuration and collected using a charge-coupled device cooled with liquid nitrogen. The resolution of the spectrometer is 1 cm^{-1}. The crystals were cooled to 30 K with an Air Products closed-cycle He refrigerator in a cryogenic chamber

 ©2009 The American Physical Society

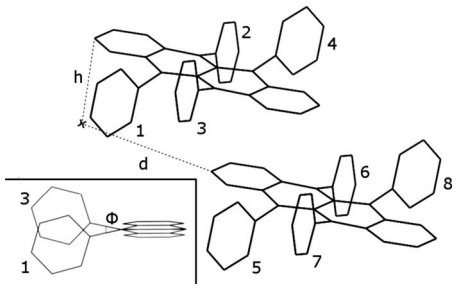

FIG. 1. Packing of two nearest-neighbor molecules in the rubrene crystal, with the hydrogen atoms hidden; inset showing torsion angle ϕ, with the backbone perpendicular to the paper.

pumped down to approximately 10^{-6} Torr with a diffusion pump vacuum system. A Spectra-Physics 2017 Ar^+ laser was used to pump a Spectra-Physics 375B dye laser with Kiton Red dye. An excitation wavelength of 650.45 nm [1.906 eV, lower than the reported rubrene band gap of 2.21 eV (Ref. 25)] was used in the experiments to minimize the photoluminescence from the sample in order to measure the weaker Raman effect. Previous work has indicated that intermolecular and some low-frequency intramolecular vibrations appeared in the low-frequency range.[22,26] Following this the data were collected focusing on the spectral range below 150 cm^{-1}. Spectra at higher frequencies were also recorded for comparison purposes. After subtracting the background, all peaks were fitted using Lorentzian line shapes with a least-squares algorithm.

The vibrational modes of the isolated rubrene molecule and the energies of pairs of molecules with different point groups were simulated using GAUSSIAN 03, with the density-functional theory (DFT) (Ref. 27) B3LYP method[28–30] and the 6-311G(d) basis set.[31,32] The calculations were performed starting from the experimental x-ray structures provided by Jurchescu,[21] on an SGI Origin 3800 with 64 CPUs and 128 GB memory running the IRIX 6.5 operating system.

III. RESULTS AND DISCUSSION

Rubrene is a molecular crystal in which the molecules are loosely bound to each other via van der Waals forces. The rubrene molecule is a relatively small aromatic hydrocarbon consisting of a backbone of four fused benzene rings (tetracene) with four substituted phenyl groups (two on each internal ring). More information about the molecule structure and unit cell can be found elsewhere.[21,26] We show in Fig. 1 the packing of two nearest-neighbor molecules in the crystal extracted directly from x-ray data at 293 K.

As can be seen, the backbone planes of the two rubrene molecules are parallel to each other, separated by a distance $h=3.74$ Å in the direction perpendicular to the plane. For each molecule, two phenyl groups attached to the same internal ring (taking 1 and 2 as the example) are below the backbone plane on one end while the two phenyl groups attached to the other ring (3 and 4) are above the plane on the other end. At room temperature (293 K), the torsion angle ϕ between side groups 1 and 3 is $\sim 25°$, and the molecular displacement d, which is defined as the distance between the ends of the two molecules projected on the plane of the tetracene backbone, is ~ 6.176 Å. A major feature of the rubrene crystal is that no change occurs in h with temperature,[33] however both ϕ and d vary with temperature. It is also worthwhile to notice that phenyl groups 3 and 5 lie on opposite sides of their respective tetracene backbones to minimize the overlap between the molecules and keep the total energy at a minimum, and similarly for groups 4 and 6.

In Fig. 2 we show our Raman results for the crystal. In Fig. 2(a), which is a comparison of Raman spectra at low temperature (30 K) and room temperature (300 K), peaks I and II only appear at low temperatures. They redshift to the lower-frequency range quickly with increasing temperature, with little change in their linewidths below ~ 80 K, above which the peaks become undetectable (below 20 cm^{-1}) with our instrument. Other peaks (III–VII) shift in position only slightly ($<3\%$), however they broaden in linewidth significantly. To examine these changes more closely, we plot the evolution of the peak positions and linewidths with temperature, and the results are presented in Figs. 2(b) and 2(c). In Fig. 2(b), the rapid shift of peaks I and II with temperature is striking. Based on this we catalog these vibrations as intermolecular vibrations, and conclude that other peaks (III–VII) come from intramolecular vibrations,[26] or the coupling between intermolecular and intramolecular vibrations.[22] In Fig. 2(c) it is notable that only the peaks below 150 cm^{-1} (III–VII) are strongly broadened with increasing temperature while higher-frequency peaks [not shown in Fig. 2(a)] broaden only gradually, e.g., those at ~ 340 and ~ 896 cm^{-1}. Further, around 150 K there is an abrupt change and the broadening begins to increase steeply, and at higher temperature the rate of increase slows down again. The spectral linewidth of a Raman peak is determined by the inverse of the lifetime of its corresponding phonon.[34] As the temperature goes up, the phonons can decay more easily into another state, thus a gradual peak broadening is expected in most crystals. In tetracene and pentacene this kind of gradual broadening was observed as well in the low-frequency range (increase of approximately a factor of 2 over $\sim 80–300$ K).[35,36] The low-frequency peaks in rubrene, i.e., III–VII as shown in Fig. 2, broaden by a factor of ~ 5 over 30–300 K, and go through an abrupt broadening at ~ 150 K. The broadening observed in rubrene is therefore much more dramatic than that observed in similar materials, and suggests that factors in addition to the usual phonon decay must be at work. Even if the peaks below 150 cm^{-1} result from coupled intermolecular and intramolecular vibrations, an abrupt change in those vibrations must occur near 150 K in order for this phenomenon to be observed in rubrene.

The massive phenyl side groups of rubrene molecules are very flexible and their motions are almost uncoupled from the backbone of the molecule,[33] thus they are responsible for the low-frequency phonons in the Raman spectra. Among these motions the one perpendicular to the backbone plane involves the smallest energy, as indicated by simulations[26] and analytical calculations.[33] It is therefore natural to conclude that the broadening of the low-frequency peaks (III–VII) is due to the shortening of the lifetime of the motion of the side groups, which results from an abrupt change in the motion perpendicular to the backbone. Here we propose a

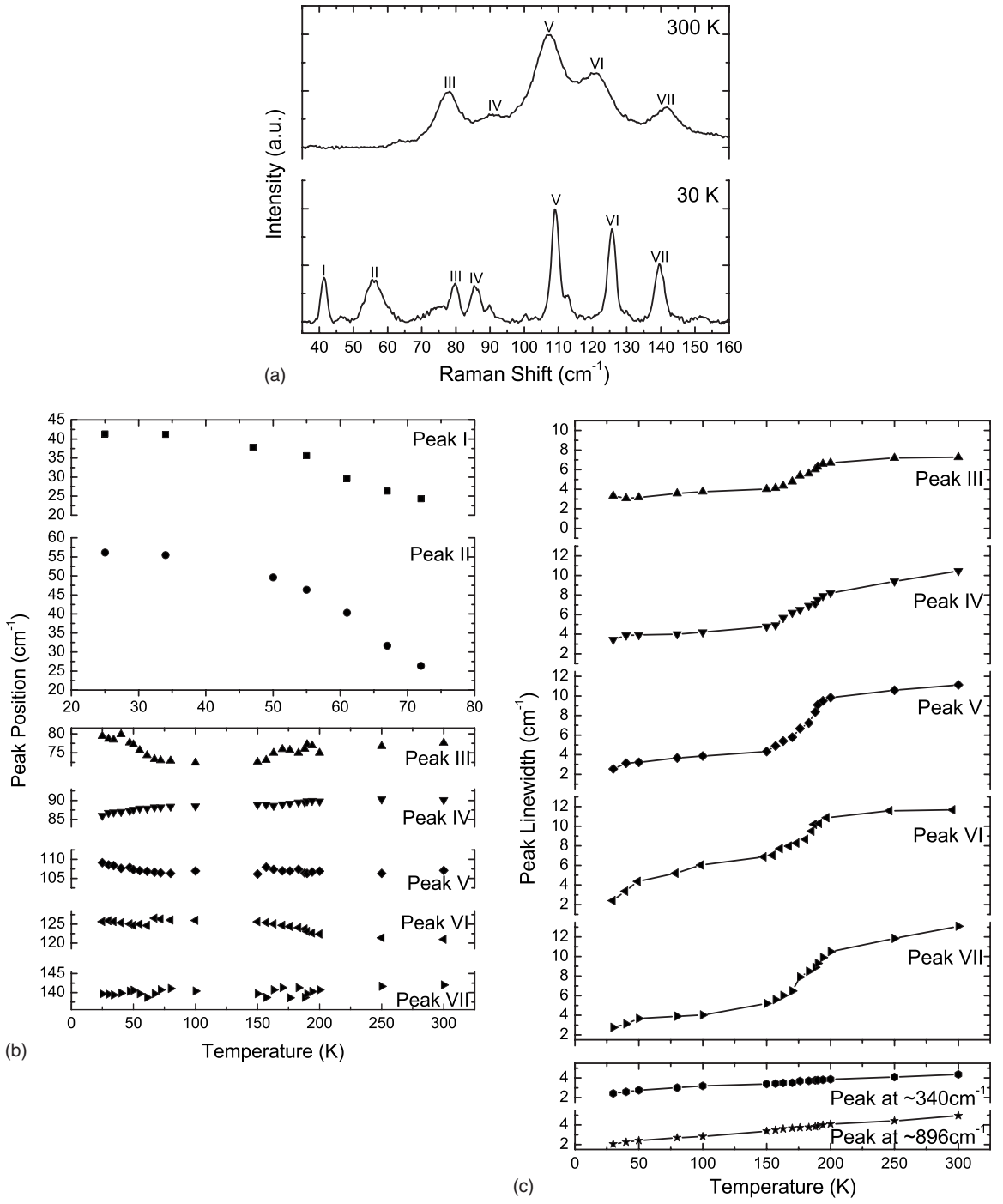

FIG. 2. (a) Comparison of Raman spectra at low temperature (30 K) and room temperature (300 K); (b) evolution of the peak positions with temperature (note the different temperature scales in the upper and lower parts of the graph); (c) evolution of the peak linewidths with temperature.

simple model to explain what we observe in Fig. 2(c), as well as other phenomena observed in this material, i.e., the changes in the mobility, thermal properties, and structure as revealed by x-ray diffraction at temperatures near ~150 K.

The model is illustrated in Fig. 3. Taking phenyl groups 1 and 3 as an example, initially they vibrate around their equilibrium positions below and above the backbone plane, respectively, and they are unable to cross the backbone plane under this circumstance [as shown in Fig. 3(a); also see in the following link animations of the vibrations for a better understanding of their motions, http://www.physics.unc.edu/project/mcneil/MolecularAnimations/anim.php (Ref. 26)]. But as the temperature goes up, phenyl groups 1 and 3 gain enough energy to go over the energy barrier, the maximum of which occurs where they are cofacial and approach each other most closely [as shown in Fig. 3(b)]. They exchange sides and set up new equilibrium positions there [as shown in Fig. 3(c)]. In the crystal other phenyl group pairs could go

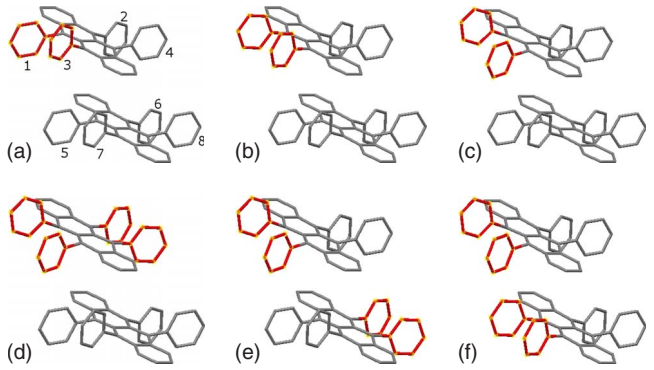

FIG. 3. (Color online) (a) Rubrene molecules in the low-energy state; (b) two phenyl groups (1 and 3) are cofacial where the maximum of the energy barrier occurs; (c) the phenyl groups have exchanged sides; [(d)–(f)] with one phenyl group pair having exchanged sides, another pair becomes cofacial simultaneously.

through this process simultaneously, and Figs. 3(d)–3(f) illustrate these situations in which the additional activated pairs are 2 and 4, 6 and 8, 5 and 7, respectively.

In order to verify our theory we calculated the energy of the two-molecule units shown in Fig. 3, with different phenyl group positions at different temperatures. We define the energy differences between Figs. 3(a) and 3(b), 3(a) and 3(d), 3(a) and 3(e), 3(a) and 3(f), as ΔE_1, ΔE_2, ΔE_3, and ΔE_4, respectively. The results are presented in Fig. 4.

In our model the ΔE's are affected by two factors: within the molecule by the torsion angle ϕ between the phenyl groups that exchange sides, and externally by the molecular displacement d between the molecules. Generally speaking, larger displacement and smaller torsion angle lead to smaller ΔE's. However, the larger torsion angle generates more overlap with, and thus repulsion of, the phenyl groups on the neighboring molecule, in which case the two molecules displace slightly with respect to each other, increasing d to keep the system energy low. Thus larger torsion angle induces a larger displacement and the two effects compete to affect the ΔE's. That is why although the molecular displacement increases monotonically with increasing temperature,[21] the energy differences do not. It is noteworthy that the torsion angle between the two phenyl groups after they have exchanged sides is smaller than in the original position; our calculation shows it to be less than ~10° (in Fig. 3 we used larger torsion angles to make the change more obvious). Thus the structure in which the phenyl groups have exchanged sides, or "flipped," as shown in Fig. 3(c), is unstable, and goes back to Fig. 3(a) easily. This "flipping" process shortens the lifetimes of the phonons and thus broadens the Raman peaks. Specifically the transition rate $1/\tau$ for the phenyl groups to cross the energy barrier is

$$1/\tau = \upsilon e^{-\Delta E/k_B T}, \tag{1}$$

where $\upsilon \sim 10^{12}$ Hz is the typical vibration frequency and ΔE is the energy barrier in the different cases. Employing the calculated ΔE's, we are able to explain in detail our Raman observations. From 30–150 K $1/\tau$ increases with temperature with a relatively large but constant ΔE_1 (since d changes only slightly); around 150 K there is a sudden decrease in the energy barrier, which increases $1/\tau$ exponentially, enabling more phenyl groups to exchange sides and enlarging the linewidths as shown in Fig. 2(c). Above 150 K ΔE_1 remains at a relatively small value but increases with temperature on average, which slows down the flipping rate. Meanwhile the increase in the number of molecules with flipped phenyl groups prevents an additional flip in the neighboring molecules [as shown in Figs. 3(d)–3(f)] since the energies needed to do so (ΔE_{2-4}) are significantly larger, as seen in Fig. 4. Such large energy barriers further slow down the flipping rate, therefore at higher temperature this effect becomes weak and the Raman peak broadening slows down.

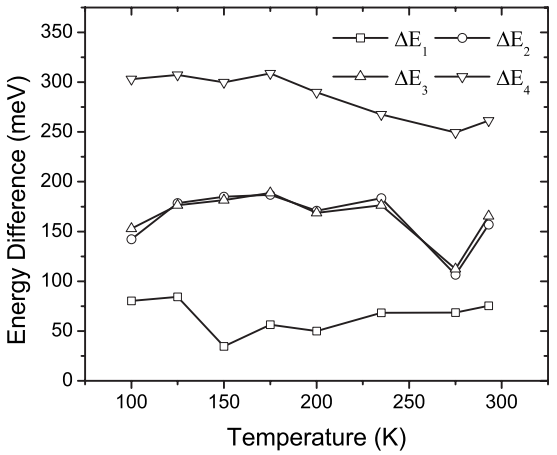

FIG. 4. Evolution of energy differences between different phenyl group positions with temperature.

Our model explains previous observations of other phenomena well, in particular, the behavior of the carrier mobility of rubrene single crystals at low temperature. We consider band transport and hopping transport, the two fundamental transport mechanisms in rubrene. In the hopping model, the rate of charge transfer (W) between neighboring molecules can be described as follows according to Marcus theory,[37,38]

$$W = \frac{2t_{mn}^2}{h}\left(\frac{\pi^3}{\lambda k_B T}\right)^{1/2} \exp\left(-\frac{\lambda}{4k_B T}\right), \tag{2}$$

where t_{mn} is the electronic coupling integral for all the molecular pairs, with m and n denoting the nearest-neighbor molecules, and λ is the sum of intramolecular and intermolecular reorganization energy for the charge carriers. The mobility μ can be directly calculated from W by the Nernst-Einstein relation through the diffusion coefficient D,[39,40]

$$D = \frac{1}{2s}\sum_i r_i^2 W_i^2, \tag{3}$$

$$\mu = \frac{e}{k_B T} D, \tag{4}$$

where s is the dimensionality of the crystal, r is the distance between the pairs of molecules, and W_i is the probability for the charge carrier to hop to a particular ith neighbor, normalized over the total hopping rate ($\Sigma_i W_i$). Equations (2)–(4) clearly suggest that smaller λ, larger t, and higher T lead to

larger μ. In rubrene, the electronic coupling is strong and a large fraction (~25%) of the intramolecular reorganization energy comes from the low-frequency vibrational modes, i.e., the motion of the phenyl side groups, as indicated by calculations at the DFT level.[33] Therefore when the phenyl group flipping eliminates these vibrations, λ is reduced accordingly and μ increases. On the other hand, in band transport with the interaction of the delocalized carriers with the phonons (the main scattering process), carrier mobility in crystals decreases with temperature according to the following equation:

$$\mu = CT^{-n}, \tag{5}$$

where C and n are constants.[19] These two effects are in competition to affect carrier mobility. At low temperature, T changes the flipping rate exponentially, and as more low-frequency vibrational modes are eliminated, λ is reduced and the hopping process becomes easier, which explains why the carrier mobility increases with temperature below 150 K. As the temperature increases, the second effect begins to dominate for charge transport. But more and more phenyl groups are activated to exchange sides in the range 150–200 K, and they enhance the hopping between neighboring molecules so μ remains nearly constant. At higher temperature, the number of flipped phenyl group pairs no longer increases significantly, as discussed above, and with band transport becoming dominant, the mobility decreases gradually with temperature. (See Ref. 5 Fig. 2 for the carrier mobility behavior in rubrene over this temperature range.) Notably, in hopping transport μ could fluctuate greatly with even a tiny change in λ, especially at low temperatures, e.g., a 1% decrease in λ causes a ~14% increase in μ at 150 K. Thus in the real situation, an increase in μ by a factor of 2–3 in the range 125–175 K, as shown in Ref. 5, is possible even in the presence of trapping. A measurement of Hall mobility in the range 100–175 K, which is independent of trapping and yields the change in free-carrier mobility with increasing temperature, would clarify the picture. We also notice that in the range 230–290 K, the Hall mobility at fixed gate voltage changes only slightly with temperature,[16] which agrees with our model.

It should be noted that this model of the relationship between the motion of the phenyl side groups and the temperature dependence of the mobility does not itself explain the unusually large mobility observed in this material. Recent work has pointed to oxidation on the crystal surface as being an important contributor to the high mobility measured in FET structures (in which the conduction is limited to a narrow channel close to the rubrene surface).[41–43] However, the phenomenon of the flipping of the phenyl groups should occur throughout both the bulk and the surface of the crystal, and therefore will influence the temperature dependence of the charge transport regardless of where the transport takes place.

Other phenomena observed in rubrene single crystals explained by this model are the differential scanning calorimetry (DSC) and x-ray results. DSC measurements showed a small bump over 155–195 K which is centered at 173 K.[21,44] That is because in this range significantly more phonons are eliminated due to the flipping effect, as seen in Fig. 2(c). This is a moderately exothermic process but not a full phase transition. On the other hand, the phenyl groups exchange sides back and forth at a very high frequency (typically $\sim 10^{12}$ Hz) while the backbones basically stay still, a process too rapid to be captured in conventional x-ray diffraction.[21]

Last but not least, our model explains why d increases with temperature.[21] Exactly as a larger torsion angle induces a larger displacement, as discussed above, the flipped phenyl groups generate overlap with, and thus repulsion of, the neighboring molecule as well. Therefore d increases to keep the system energy low. The displacement change then affects the further flipping through the energy barriers, as discussed above.

Our model has several important implications for future NMR and x-ray studies. Above 150 K phenyl groups that exchange sides at rates exceeding the chemical shift anisotropy will experience motional narrowing and would be easily distinguished from the stationary backbone spectrum. In addition, a detailed examination of the Debye-Waller factor around 150 K would clarify how the flipping-induced disorder affects the x-ray diffraction pattern. Further, although below room temperature the flipping is an intermittent phenomenon, there could exist a higher temperature above which the phenyl groups could exchange sides back and forth freely. As the temperature goes up, precursors of this "free flipping" transition might be observed in the above-mentioned measurements, e.g., a sudden narrowing of the NMR peaks, or an abnormal attenuation of x-ray scattering. Finally, a similar effect might also be observable in other materials whose molecules have massive but flexible side groups and are loosely bound to each other, e.g., a rubrene derivative, 5,12-Bis(4-tert-butylphenyl)-6,11-diphenylnaphthacene (5,12-BTBR).[45]

IV. CONCLUSION

In conclusion, we report Raman spectra of rubrene single crystals in the temperature range 30–300 K. The Raman peaks of certain low-frequency vibration modes are greatly broadened as the temperature increases, especially in the range 150–200 K. We have constructed a simple model to describe the motions of massive phenyl side groups of rubrene molecules, which explains our Raman observation as well as other important phenomena observed in crystalline rubrene. DFT calculations have also been performed to support the theory. Starting from the model we discuss possible temperature-dependent NMR and x-ray properties of the material.

ACKNOWLEDGMENTS

Z.Q.R. and L.E.M. would like to thank Oana Jurchescu for sharing her original x-ray data. Z.Q.R. acknowledges John Hernandez, Jianping Lu, Lu-chang Qin, and Alfred Kleinhammes, as well as Hai-jing Wang for helpful discussions. This work is supported by the National Science Foundation through Grant No. DMR-0505773.

*zqren@physics.unc.edu

[1] C. W. Tang and S. A. VanSlyke, Appl. Phys. Lett. **51**, 913 (1987).
[2] G. Horowitz, F. Garnier, A. Yassar, R. Hajlaoui, and F. Kouki, Adv. Mater. (Weinheim, Ger.) **8**, 52 (1996).
[3] Zhang Zhilin, Jiang Xueyin, and Xu Shaohong, Thin Solid Films **363**, 61 (2000).
[4] H. Aziz and Z. D. Popovic, Appl. Phys. Lett. **80**, 2180 (2002).
[5] V. Podzorov, E. Menard, A. Borissov, V. Kiryukhin, J. A. Rogers, and M. E. Gershenson, Phys. Rev. Lett. **93**, 086602 (2004).
[6] C. Reese and Z. N. Bao, Mater. Today **10**, 20 (2007).
[7] R. W. I. de Boer, M. E. Gershenson, A. F. Morpurgo, and V. Podzorov, Phys. Status Solidi A **201**, 1302 (2004).
[8] M. Uchida, C. Adachi, T. Koyama, and Y. Taniguchi, J. Appl. Phys. **86**, 1680 (1999).
[9] E. Botzung-Appert, V. Monnier, T. Ha Duong, R. Pansu, and A. Ibanez, Chem. Mater. **16**, 1609 (2004).
[10] A. S. Arutyunov, Instrum. Exp. Tech. **25**, 769 (1982).
[11] G. Sakamoto, C. Adachi, T. Koyama, Y. Taniguchi, C. D. Merritt, H. Murata, and Z. H. Kafafi, Appl. Phys. Lett. **75**, 766 (1999).
[12] Y. Hamada, H. Kanno, T. Sano, H. Fujii, Y. Nishio, H. Takahashi, T. Usuki, and K. Shibata, Appl. Phys. Lett. **72**, 1939 (1998).
[13] E. Menard, V. Podzorov, S. H. Hur, A. Gaur, M. E. Gershenson, and J. A. Rogers, Adv. Mater. (Weinheim, Ger.) **16**, 2097 (2004).
[14] J. Takeya, M. Yamagishi, Y. Tominari, R. Hirahara, Y. Nakazawa, T. Nishikawa, T. Kawase, T. Shimoda, and S. Ogawa, Appl. Phys. Lett. **90**, 102120 (2007).
[15] S. Ono, K. Miwa, S. Seki, and J. Takeya, Appl. Phys. Lett. **94**, 063301 (2009).
[16] J. Takeya, J. Kato, K. Hara, M. Yamagishi, R. Hirahara, K. Yamada, Y. Nakazawa, S. Ikehata, K. Tsukagoshi, Y. Aoyagi, T. Takenobu, and Y. Iwasa, Phys. Rev. Lett. **98**, 196804 (2007).
[17] O. D. Jurchescu, J. Baas, and T. T. M. Palstra, Appl. Phys. Lett. **84**, 3061 (2004).
[18] T. Siegrist, C. Kloc, J. H. Schon, B. Batlogg, R. C. Haddon, S. Berg, and G. A. Thomas, Angew. Chem., Int. Ed. **40**, 1732 (2001).
[19] K.-C. Kao, *Electrical Transport in Solids* (Pergamon, New York, 1981), Vol. 14.
[20] U. Sondermann, A. Kutoglu, and H. Bassler, J. Phys. Chem. **89**, 1735 (1985).
[21] O. D. Jurchescu, A. Meetsma, and T. T. M. Palstra, Acta Crystallogr., Sect. B: Struct. Sci. **62**, 330 (2006).
[22] E. Venuti, I. Bilotti, R. G. Della Valle, A. Brillante, P. Ranzieri, M. Masino, and A. Girlando, J. Phys. Chem. C **112**, 17416 (2008).
[23] Z. Q. Li, V. Podzorov, N. Sai, M. C. Martin, M. E. Gershenson, M. Di Ventra, and D. N. Basov, Phys. Rev. Lett. **99**, 016403 (2007).
[24] R. Zeis, C. Besnard, T. Siegrist, C. Schlockermann, X. L. Chi, and C. Kloc, Chem. Mater. **18**, 244 (2006).
[25] Y. Hamada, H. Kanno, T. Tsujioka, H. Takahashi, and T. Usuki, Appl. Phys. Lett. **75**, 1682 (1999).
[26] J. R. Weinberg-Wolf, L. E. McNeil, S. Liu, and C. Kloc, J. Phys.: Condens. Matter **19**, 276204 (2007).
[27] R. G. Parr and W. Yang, *Density-Functional Theory of Atoms and Molecules* (Oxford University Press, Oxford, UK, 1989).
[28] A. D. Becke, Phys. Rev. A **38**, 3098 (1988).
[29] A. D. Becke, J. Chem. Phys. **98**, 5648 (1993).
[30] C. Lee, W. Yang, and R. G. Parr, Phys. Rev. B **37**, 785 (1988).
[31] R. Krishnan, J. S. Binkley, R. Seeger, and J. A. Pople, J. Chem. Phys. **72**, 650 (1980).
[32] M. J. Frisch, J. A. Pople, and J. S. Binkley, J. Chem. Phys. **80**, 3265 (1984).
[33] D. A. da Silva Filho, E.-G. Kim, and J. L. Brédas, Adv. Mater. (Weinheim, Ger.) **17**, 1072 (2005).
[34] M. T. Dove, *Introduction to Lattice Dynamics* (Cambridge University Press, New York, 1993).
[35] E. Venuti, R. G. Della Valle, L. Farina, A. Brillante, M. Masino, and A. Girlando, Phys. Rev. B **70**, 104106 (2004).
[36] R. G. Della Valle, E. Venuti, L. Farina, A. Brillante, M. Masino, and A. Girlando, J. Phys. Chem. B **108**, 1822 (2004).
[37] R. A. Marcus, J. Chem. Phys. **24**, 966 (1956).
[38] R. A. Marcus, Rev. Mod. Phys. **65**, 599 (1993).
[39] W. Q. Deng and W. A. Goddard, J. Phys. Chem. B **108**, 8614 (2004).
[40] S. Mohakud and S. K. Pati, J. Mater. Chem. **19**, 4356 (2009).
[41] W. Y. So, J. M. Wikberg, D. V. Lang, O. Mitrofanov, C. L. Kloc, T. Siegrist, A. M. Sergent, and A. P. Ramirez, Solid State Commun. **142**, 483 (2007).
[42] C. Krellner, S. Haas, C. Goldmann, K. P. Pernstich, D. J. Gundlach, and B. Batlogg, Phys. Rev. B **75**, 245115 (2007).
[43] O. Mitrofanov, C. Kloc, T. Siegrist, D. V. Lang, W. Y. So, and A. P. Ramirez, Appl. Phys. Lett. **91**, 212106 (2007).
[44] O. D. Jurchescu, Ph.D. thesis, University of Groningen, 2006.
[45] G. Schuck, S. Haas, A. F. Stassen, H. J. Kirner, and B. Batlogg, Acta Crystallogr. Sect. E: Struct. Rep. Online **63**, o2893 (2007).